J. Membrane Biol. 166, 133–147 (1998)

The Journal of
Membrane
Biology

A New Structural Model for P-Glycoprotein

P.M. Jones, A.M. George
Department of Cell and Molecular Biology, University of Technology Sydney, Sydney, NSW 2007, Australia

Received: 18 February 1998/Revised: 2 September 1998

Abstract. Multidrug resistance to anti-cancer drugs is a major medical problem. Resistance is manifested largely by the product of the human *MDR1* gene, P-glycoprotein, an ABC transporter that is an integral membrane protein of 1280 amino acids arranged into two homologous halves, each comprising 6 putative transmembrane α-helices and an ATP binding domain. Despite the plethora of data from site-directed, scanning and domain replacement mutagenesis, epitope mapping and photoaffinity labeling, a clear structural model for P-glycoprotein remains largely elusive. In this report, we propose a new model for P-glycoprotein that is supported by the vast body of previous data. The model comprises 2 membrane-embedded 16-strand β-barrels, attached by short loops to two 6-helix bundles beneath each barrel. Each ATP binding domain contributes 2 β-strands and 1 α-helix to the structure. This model, together with an analysis of the amino acid sequence alignment of P-glycoprotein isoforms, is used to delineate drug binding and translocation sites. We show that the locations of these sites are consistent with mutational, kinetic and labeling data.

Key words: P-glycoprotein — Membrane topology — Multidrug resistance — β-barrel — ABC transporter

Introduction

Multidrug resistance (MDR) in cancer patients or in tissue cultured cancer cells is manifested primarily as cross resistance to structurally and functionally unrelated chemotherapeutic drugs following treatment with a single drug. The best characterized MDR system is that mediated by the product of the human *MDR1* gene, P-glycoprotein (Pgp), a 170 kDa integral membrane protein (Juliano & Ling, 1976) whose diverse range of substrates includes natural product drugs, immunosuppressive and antifungal agents, peptide antibiotics and steroid hormones (Endicott & Ling, 1989; Gottesman & Pastan, 1993; Kane, 1996; Germann, 1996). Human Pgp (MDR1) is 1280 amino acids arranged in two homologous halves with each half comprising 6 putative transmembrane (TM) α-helices and an ATP-binding domain. Pgp isoforms have greater than 70% sequence identity and are encoded by a small family of closely-related genes which has three members in mice (*mdr1, mdr2, mdr3*), two in rats (*mdr1* and *mdr2*), three in hamsters (*pgp1, pgp2, pgp3*) and two in humans (*MDR1, MDR2*) (Germann, 1996). In addition, there are many homologues in humans and other animals, insects, yeasts, and bacteria (van Veen et al., 1996). Collectively, Pgps are members of a large class of ATP-dependent transport proteins known as the ABC superfamily (Hyde et al., 1990; Mimura, Holbrook & Ames, 1991; Higgins, 1995) that regulate the trafficking of diverse molecules across biological membranes. In the recent report of the complete genome sequence of *E. coli* K-12, at least 80 ABC proteins were identified (Blattner et al., 1997), and ABC transporters make up one of the four major gene families in humans (Tatusov, Koonin & Lipman, 1997). Within the ABC transporter family, Pgp, MRP, five yeast ABC proteins and LmrA (from *Lactococcus lactis*) are known to have broad substrate specificities. The mechanism by which Pgp couples ATP energy to the translocation and efflux of a diverse range of substrates is largely an unresolved debate (reviewed in Kane, 1996; Germann, 1996; Ruetz & Gros, 1994; Gottesman et al., 1995; Bolhuis et al., 1997). Although a considerable body of biochemical and genetic data has accrued for Pgp and many other ABC transporters, it is generally agreed that further progress in the understanding of the molecular mechanisms of active transport is limited by the lack of structural information (Rosenberg et al., 1997).

Correspondence to: A.M. George

The most widely accepted model (Juranka, Zastawny & Ling, 1989) for the human Pgp isoform (MDR1) was derived by comparison of the hydropathy profile with those of membrane proteins proposed to contain transmembrane α-helices, such as bacteriorhodopsin. This model displays two homologous halves with each having 6 TM α-helices and a nucleotide binding domain (NBD). Notwithstanding its wide currency, and despite an intensive effort which has produced a vast body of data, this 6 + 6 helix model for Pgp has not been developed since it was first proposed over 8 years ago. Indeed, the few predictions made by the model have proven difficult to verify with mapping experiments yet to confirm the topology. Although the sequences embodying the putative TM helices are clearly delimited by an hydropathy prediction, no possible scheme of their arrangement has been found. The Pgp molecule thus has been difficult to analyze, and the 6 + 6 helix model has proven to be an essentially unyielding template not only for the understanding of Pgp, but for many other ABC transporters as well (Fischbarg et al., 1994).

The 6 + 6 helix model has been challenged (Fischbarg et al., 1993), as has the legitimacy of comparisons of membrane transporters with bacteriorhodopsin (Raussens, Ruysschaert & Goormaghtigh, 1997). Recent infrared spectroscopic analyses of the secondary structure of other membrane transporters have contradicted predictions based on the hydropathy profile, and have unexpectedly revealed that the membrane spanning domains of these proteins contain substantial β-structure (Gorne-Tschelnokow et al., 1994; Raussens et al., 1997). In this report, we propose a new structural model for Pgp that is suggested by computer prediction algorithms, the hydropathic profile and secondary structure analysis, and is supported by previous data from residue replacement mutagenesis, epitope mapping and photoaffinity labeling. This alternative model fits the data better than the previous model, and importantly, provides a detailed template for positioning and interpreting mutations. This new topological model might also have utility as a general structure for other ABC transporters. The expression of human Pgp in *E. coli* (George, Davey & Mir, 1996) provides an ideal system for testing the new model.

Materials and Methods

The hydropathy profiles were generated from the original computer prediction (Kyte & Doolittle, 1982) using the software program DNA Strider. The distribution of aromatic residues on the ends of predicted β-strands was subjected to a Chi-squared test [$\chi^2 = \Sigma(O - E)^2/E$] for statistical significance. Observed (O) values were taken as the number of aromatic (27) and non-aromatic (37) residues on the 64 ends of the 32 putative TM β-strands. There were 48 aromatic residues within the 32 β-strands comprising a total of 226 residues. If the distribution of aromatic residues were random, the expected (E) values would be {(48/226) × 64 = 14} for aromatic residues, and (64 − 14 = 50) for nonaromatic residues, that would be present on the ends of β-strands.

The human MDR1 P-glycoprotein amino acid sequence was analyzed with the following secondary structure computer prediction algorithms: SSPRED (Mehta, Heringa & Argos, 1995); SSP (segment oriented secondary structure prediction) (Solovyev & Salamov, 1994); nnSSP (nearest neighbor secondary structure prediction) (Salamov & Solovyev, 1995); PHDsec (Rost & Sander, 1993) and PHDacc (Rost & Sander, 1994); BMERC (Stultz, White & Smith, 1993; White, Stultz & Smith, 1994); SOPMA predict which gives a consensus of 4 prediction methods (Geourjon & Deleage, 1994; Geourjon & Deleage, 1995); and the Chou-Fasman propensity rules (Chou & Fasman, 1973).

Protein sequences were obtained from the SWISS-PROT Database at the National Centre for Biotechnology Information (NCBI). Their accession numbers and percentage identities relative to MDR1 are: Human MDR1 (P08183, 100%); Murine Mdr3 (P21447, 87%); Hamster PgpI (P21448, 87%); Hamster Pgp2 (P21449, 80.8%); Murine Mdr1 (P06795, 80.3%); Rat Mdr1 (P43245, 80.2%); Human MDR2 (P21439, 75.6%); Murine Mdr2 (P21440, 75.2); Hamster Pgp3 (P21374, 74.5%); Rat Mdr2 (Q08201, 74.4%).

The multiple protein sequence alignment was obtained using ClustalW (Thompson, Higgins & Gibson, 1994).

Abbreviations

Pgp, P-glycoprotein; MDR, multidrug resistance; MDR1, P-glycoprotein from the human *MDR1* gene; TM, transmembrane; NBD, nucleotide binding domain; NBF, nucleotide binding fold.

Results and Discussion

Hydropathy Plots and the P-glycoprotein Structural Model

At present, the detailed structures of a few membrane proteins have revealed two folding patterns — multi-α-helical and β-barrel. Approximately 20 residues in an α-helical conformation are needed to span the lipid bilayer, while for β-strands usually 9–10 residues are required, but as few as 5 residues may suffice (Cowan & Rosenbusch, 1994). The difficulty in crystallizing membrane proteins has meant that topology is assigned largely on computer predicted hydropathy plots. Although it has been suggested that reliance only on wide windows to detect long hydrophobic α-helical segments could result in erroneous structure predictions (Cowan & Rosenbusch, 1994; Ferenci, 1989), hydropathy analysis of ABC transporters has by and large failed to consider the possibility of TM β-strands.

The most widely accepted model (Juranka et al., 1989) for the human Pgp isoform (MDR1) was derived originally from the hydropathy profile. Some of the deficiencies of this topology are: (i) the weak hydropathy peaks for TMs 3, 9 and 11, and to a lesser extent TMs 4 and 7, even at an amino acid window setting of greater than 11 residues; (ii) the occurrence of prolines incongruously near the centers of TMs 1, 4, 7 and 10, although

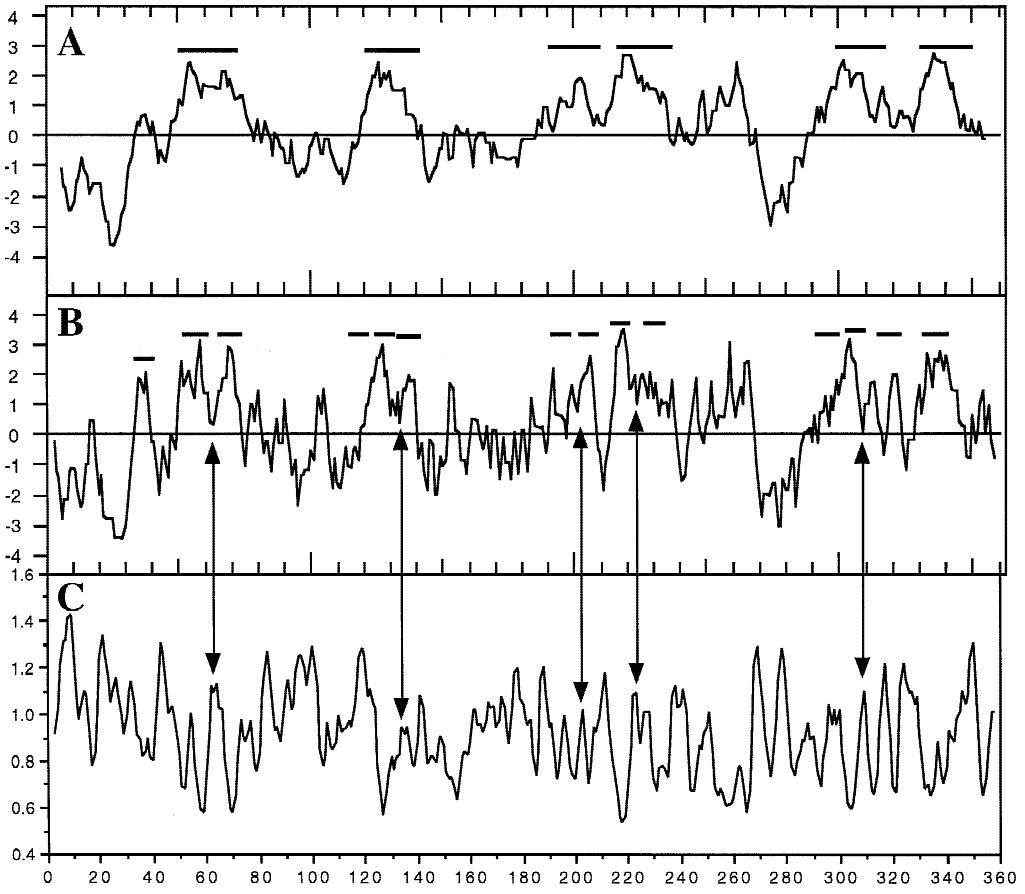

Fig. 1. Hydropathy plots and turn propensity of the N-terminal half of MDR1. The Kyte-Doolittle plots were drawn with a window of 11 (panel *A*) or 5 (panel *B*). The horizontal bars in panel *A* represent the putative α-helical TMs in the original topological model; and the shorter bars in panel *B* represent the putative β-strands in the alternative model proposed in this study. The amino acid number is given on the horizontal axes and the amphipathicity (panels *A* and *B*) or turn propensity (panel *C*) on the vertical axes. Panel *C* is a plot of the Chou and Fasman (1973) turn propensity of residues (window of five). The five double-arrowed vertical bars depict the correspondence of Chou-Fasman turns (panel *C*) with some of the predicted β-turns in the narrow window plot (panel B), and the superimposition of these turns within the five proposed α-helical TMs of the broad window plot (panel *A*).

a role for TM prolines in membrane transporters has been proposed (Deber, Glibowicka & Woolley, 1990), despite the inherent structural instability; and (iii) the fact that the assignment of some of the TMs is not consistent with the internal sequence homology of the molecule (van der Bliek et al., 1988). Hydropathy analysis of porins, whose structures are known to contain mainly secondary β-strands, reveals profiles of intermediate hydrophobicity whose broad peaks at a window of 11 residues split into narrower peaks at windows of 7 or 5 (*data not shown*). This splintering is caused by short hydrophilic turns which link pairs of largely amphipathic TM β-strands in porins. The hydropathy profile of Pgp displays TM peaks that also split at windows of 7 and 5 (Fig. 1, panels *A* and *B*). The hydropathy profile in panel *B* with a larger number of narrower peaks (Fig. 1, panel *B*) is supported by the Chou and Fasman (1973) turn propensity profile (Fig. 1, panel *C*).

Is P-glycoprotein a Double β-barrel?

There was generally strong consensus from the 10 different computer predictions for extensive α-helical structure within the two large intracytoplasmic loops between pairs of TM spans in each half of the 6 + 6 helix model of Pgp. Although there was less consensus in the secondary structure prediction of the hydrophobic TM spans, there was, nevertheless, a clearly discernible pattern of predicted β-structure and turn propensity which was consistent — in terms of lengths of β-strands and frequency of turns — with the existence of transmembrane β-barrels (Fig. 2). The positions of the predicted turns within these hydrophobic regions coincided with the short hydrophilic segments revealed by the narrow window hydropathy profiles reported above (Fig. 1, panels *B* and *C*, vertical arrows), consistent with the existence of short hydrophilic turns linking TM β-strands.

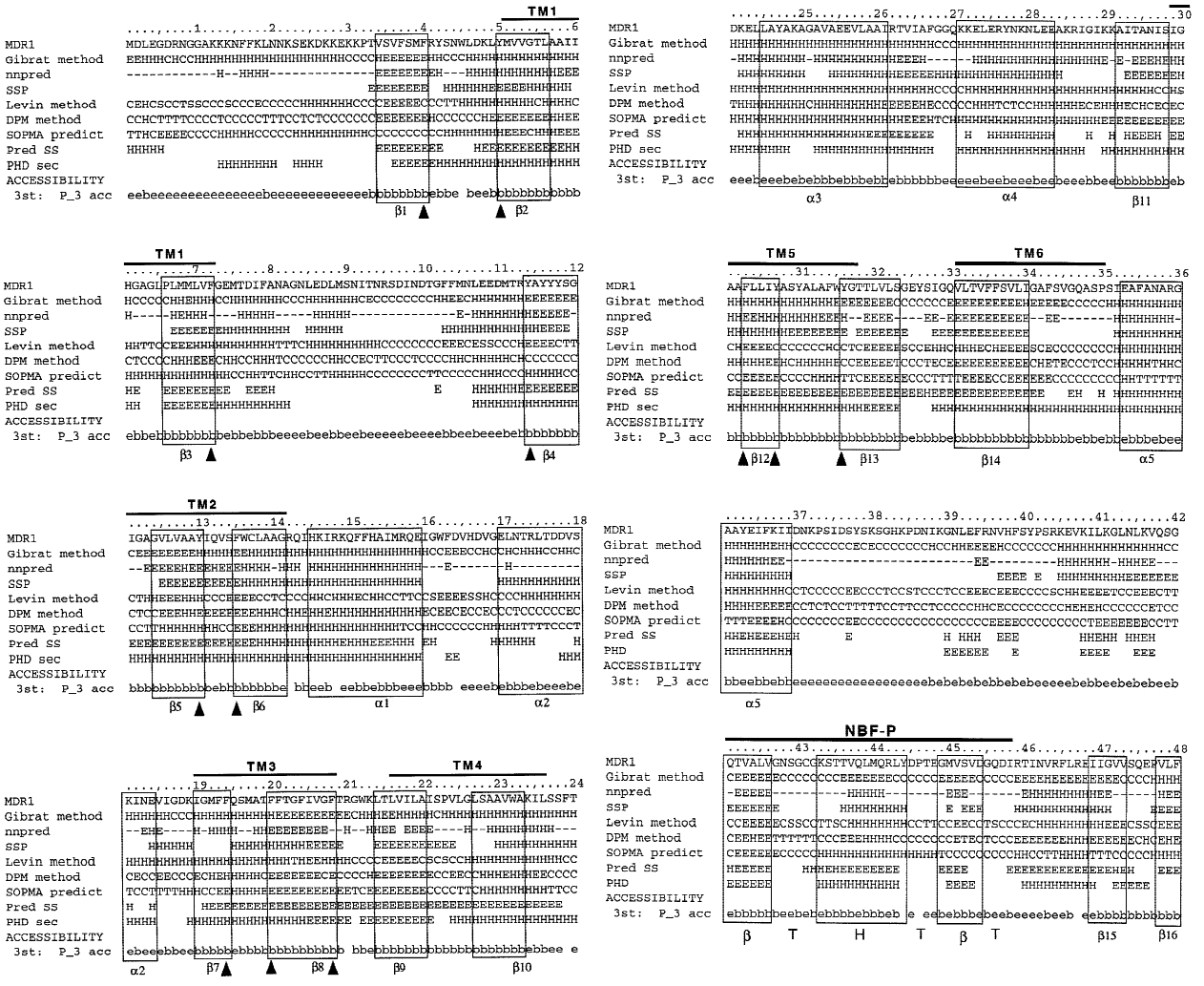

Fig. 2. Alignment of secondary structure predictions for MDR1. An alignment of the output from eight computer prediction algorithms for the secondary structure of human MDR1. The symbols are: H, α-helix; E, β-strand; C, T, S, -, or a space indicate a prediction of a loop or turn. The boxes indicate the regions interpreted as TM β-strands or intracytoplasmic α-helices as labeled below the boxes. The putative TM α-helices of the 6 + 6 helix model are indicated by overbars labeled TM followed by their number. Black arrowheads indicate residues with aromatic side chains occurring at the ends of TM β-strands. The consensus nucleotide binding folds in each half (Mimura et al., 1991) are indicated by thick overbars and are labeled NBF-P and NBF-R (*see* text). The bottom line in each row indicates the PHD solvent accessibility prediction where 'e' denotes exposed and 'b' denotes buried.

The solvent accessibility prediction and pattern of residues that potentially may form turns within the TM regions (Fig. 2), supported the correlation between the narrow hydropathy profile and turn propensity. By comparing and combining the information from the hydropathy profile and secondary structure predictions, we were able to propose a new topological model for MDR1 (Fig. 3). Each half molecule is comprised of 14 anti-parallel TM β-strands and 5 intracellular α-helices. We propose also that each ATP domain contributes two more β-strands and 1 α-helix to the structure which enables each half of the protein to be assembled as a 16 β-sheet TM barrel connected to a 6 α-helix bundle by short loops, shown in the fully extended state in Fig. 4. We have assigned 2 β-strands (β-15 and β-16) in each half of the molecule from part of the non-conserved loop between the Walker A and B motifs of the ATP domains (Fig. 3). These two strands are indicated in the computer predictions, and appear as two short nonpolar peaks in the NBD regions of the hydropathy plot of MDR1 (*not shown*). In the 6 + 6 helix model for Pgp, the helix pairs TM2/TM8 and TM5/TM11 do not occur in overlapping regions of the two homologous halves of the molecule; instead, they have been shifted relative to the internal sequence homology, according to the hydropathy profile prediction (Kyte & Doolittle, 1982). In contrast, all of the β-strands of the two halves of Pgp are in register with one another.

The proposition that the 6 α-helices in each half

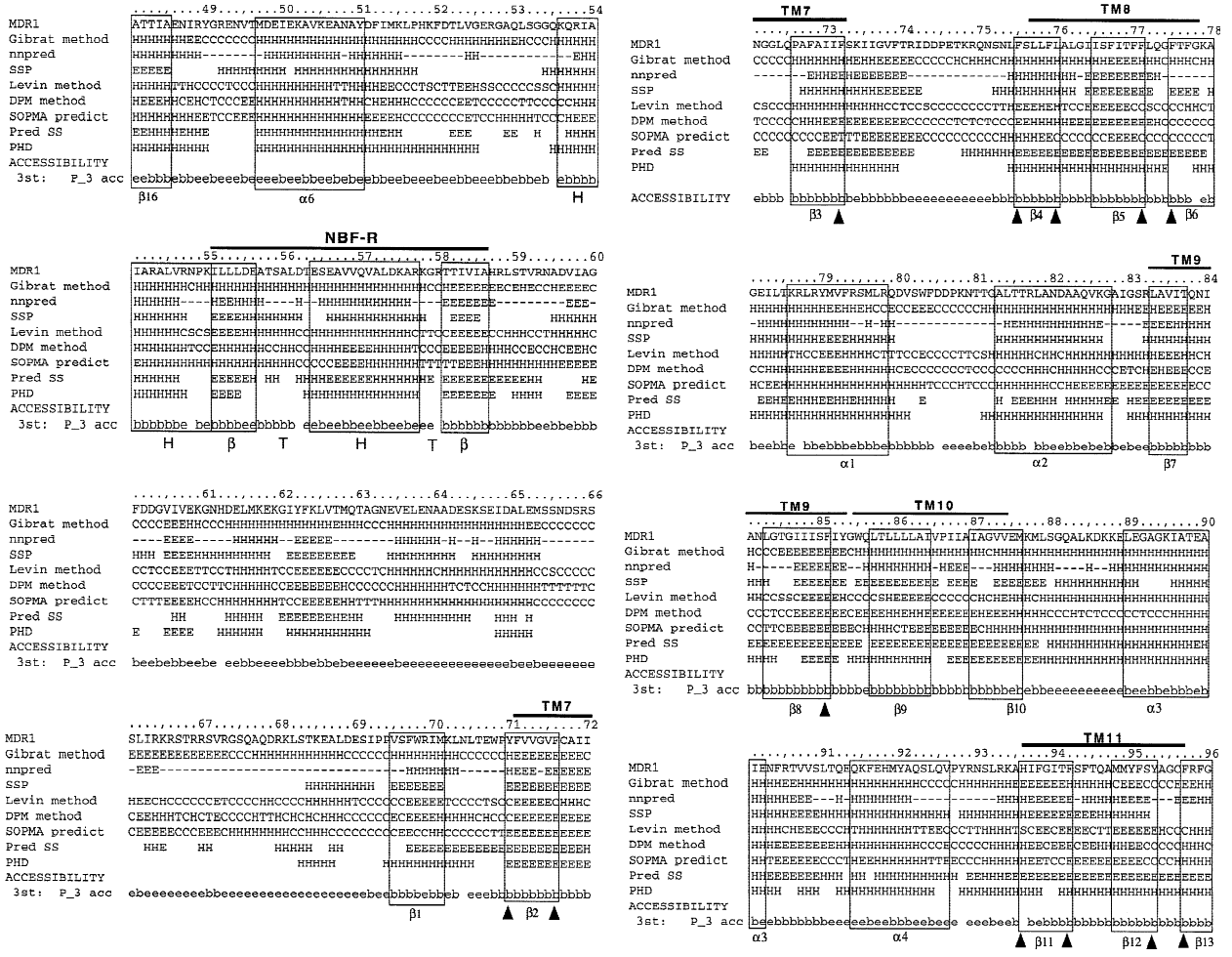

Fig. 2. Continued.

of the molecule are arranged into bundles is supported by examining the polar and nonpolar distributions around the drawn helical wheels. Figure 5 shows a deployment of the 6 helical wheels in each half of MDR1, with α-3 as the core helix and the other 5 arranged around it in the number order shown. This arrangement allows for a largely polar bundle perimeter and nonpolar interior, which together with the predicted salt bridges between the helices, would assist in stabilizing the bundle. Although the indicated salt bridges are either at the same or within one pitch length in adjacent helices, their contribution to the stabilization of the bundles is secondary to the combination of other interactions. Alanine and glycine residues frequently occur on the solvent exposed faces of helices in globular proteins and hence are shaded accordingly in Fig. 5.

It has been found that charged residues are often located immediately outside the membrane where they are associated with the negative phospholipid head groups in the bilayer or with cations that interact with them (Cowan et al., 1992). Of the 32 β-strands in our Pgp topology, 28 contain charged residues adjacent to one or both ends of the strands. It has also been found that aromatic residues tend to occupy the first position at the beginning or end of a given strand in a transmembrane β-barrel (Cowan & Rosenbusch, 1994; Song et al., 1996). Twenty-seven aromatic residues occupy delimiting positions among the 32 TM β-strands modeled (Fig. 2; arrowheads). Fifteen of these occur on either side of β-turns modeled from within some of the TM α-helical spans of the 6 + 6 model. An analysis of the aromatic amino acid content of the TM helices of Pgp showed that these residues are highly conserved (Pawagi et al., 1994). The aromatic content of the two β-barrels is 48/226 residues or 25.3% (*vs.* 18.6% for the 6 + 6 helix model), with 27 of these residues predicted to lie at the ends of β-strands (Fig. 2). Using a Chi-squared test, the observed versus expected occurrence of aromatic residues at the ends of strands was statistically significant with P between 0.01 and 0.001. It has been suggested that the distribution of aromatic residues within the TM helices is random (Pawagi et al., 1994), but with the exception of

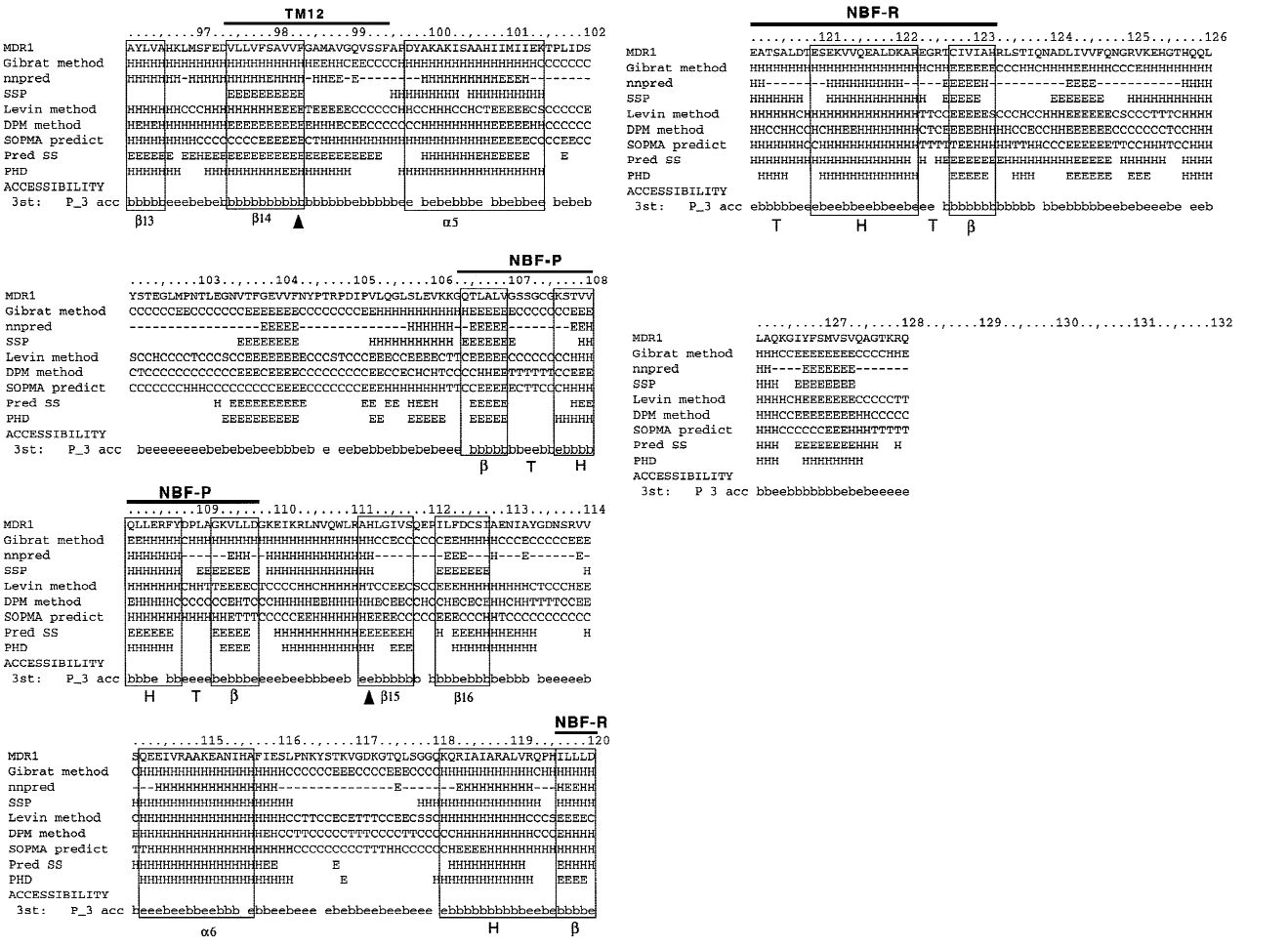

Fig. 2. Continued.

TM4 only, the other eleven TMs contain internal aromatic residues that are proposed to lie at the ends of many of the β-strands in the new model (Fig. 2).

We propose that this β-barrel/α-helix bundle structure is related to that of porins, in which mobile loops fold into the transmembrane channel and act as gating and ligand binding sites (Cowan et al., 1992; Schirmer et al., 1995; Stathopoulos, 1996). In porins, residues lining the lumen of the channel which make contact with these loops tend to be hydrophobic (Schirmer & Cowan, 1993). By analogy, this would explain the largely hydrophobic nature of the interior of the TM β-barrels revealed by our analysis of Pgp; and that has also been proposed for the interior of the channel in the 6 + 6 helix model (Pawagi et al., 1994). The hydrophobic interior of the proposed β-barrels is consistent with the transport of hydrophobic compounds through the interior of the β-barrels.

The Nucleotide Binding Domains

The ATP binding domains of ABC transporters have been modelled independently on the known structure of adenylate kinase (Hyde et al., 1990; Mimura et al., 1991), and these models are in substantial agreement (Higgins, 1992). The core of the models is a highly conserved nucleotide binding fold (NBF), consisting of two parts: A phosphate binding region which includes the Walker A motif, and the Rossman or dinucleotide-binding fold which includes the Walker B motif. Extending from this core is a large loop of about 110 residues which has no direct counterpart in adenylate kinase, is not well conserved in ABC transporters, and is thought to be responsible for transmitting the conformational changes which couple ATP hydrolysis to transport function (Mimura et al., 1991; Higgins, 1992). The configuration of this region in the new model is consistent with this function. The N-terminal half of this non-conserved loop includes a putative buried or hydrophobic helix, thought to interact with the membrane spanning complex (Mimura et al., 1991). We propose instead that part of this hydrophobic region forms two membrane spanning β-strands (β-15 and β-16, Fig. 3), which are composite components of each β-barrel, a topology that is supported by two short nonpolar peaks in the hydropathy

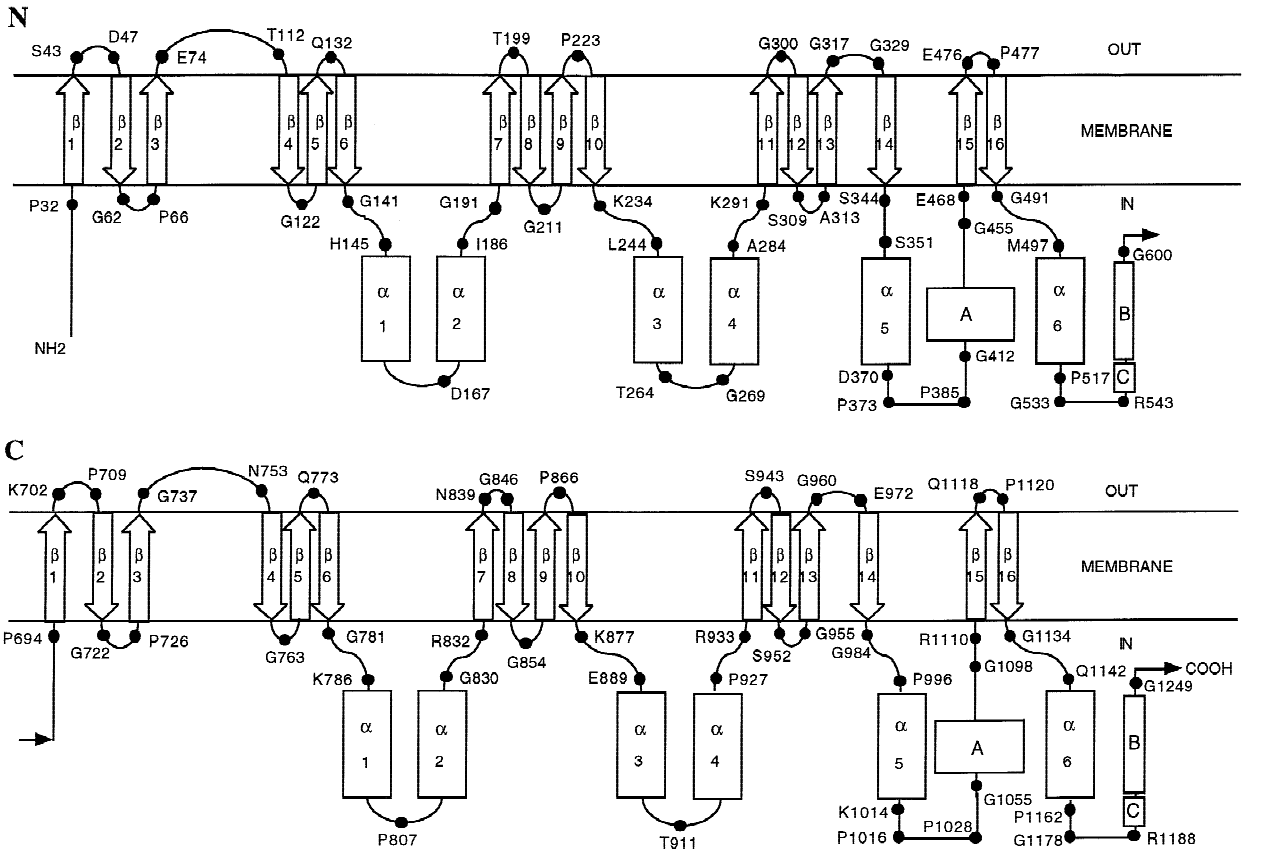

Fig. 3. An alternative topological model for human MDR1. The drawing depicts the N- and C-terminal halves of Pgp with the arrowed rectangles as membrane spanning antiparallel β-strands and the rectangles below as helical segments. The Walker A motif, the Rossman fold including the Walker B motif and the C linker dodecapeptide motif are indicated by the boxes lettered A, B and C, respectively. The numbered residues are coordinate signposts for the topology. This model is assembled as a cartoon in Fig. 4.

plot and secondary structure and solvent accessibility predictions (Fig. 2). The remainder of this non-conserved region is configured as loop-helix(α-6)-loop (Fig. 3). The C-terminal end of α-6 is thus directly connected to the Rossman fold by a short region which includes the conserved C motif or dodecapeptide linker, enabling direct mechanical coupling of the helix bundles to the NBFs (Figs. 3 and 4).

A new model of the NBDs of ABC transporters based on the crystal structure of aspartate aminotransferase has been proposed (Hoedemaeker, Davidson & Rose, 1998). One of the advantages claimed for this model is that it predicts the structure of the non-conserved loop. This new homology model differs from our modeling of part of the non-conserved loop (residues 470–505, MDR1), which includes the hydrophobic region of β-strands 15 and 16. The authors note, however, that in this region their alignment is not optimal, and it is also notable that the quality of the model, as assessed by two structure verification programs, is poor in this same region (residues 470-490, MDR1).

Infrared Spectroscopy and Electron Microscopy for P-glycoprotein and Related Membrane Proteins

A quantitative evaluation of the secondary structure of MDR1 was reported recently using attenuated total reflection Fourier transform infrared spectroscopy (Sonveaux et al., 1996). This study produced a secondary structure composition of 32% α-helix, 26% β-sheet, 29% β-turns and 13% random coil. If the TM regions were largely α-helical, then there would need to be extensive β-structure within the intracytoplasmic regions to account for the calculated 26% β-sheet. This would require that the pattern of hydrophobicity and connections revealed by the helical wheel representation depicted in Fig. 5 is merely coincidental, and this seems unlikely. Conversely, if our modeling of the helix bundles and TM spans is correct (Fig. 3), together with the previous modelling of the NBDs (Mimura et al., 1991), then our calculated totals for almost the whole of the Pgp molecule are 29% α-helix and 24% β-sheet, which are in good

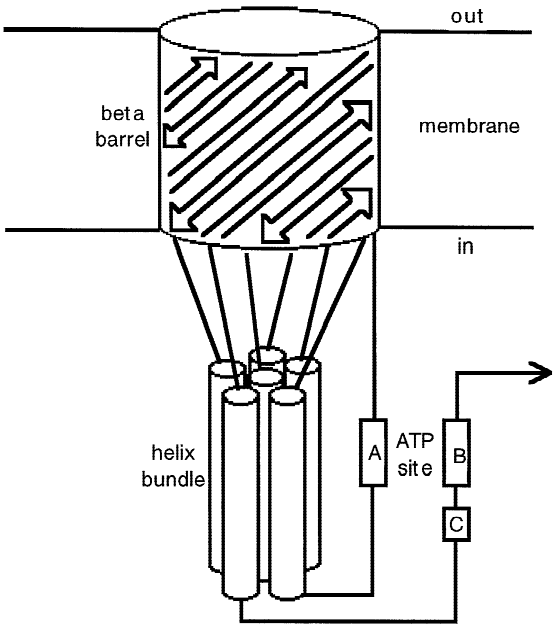

Fig. 4. Proposed assembly of the N-terminal half of MDR1. The structure is drawn as a cartoon to illustrate the proposed assembly and interaction of the β-barrel, helix bundle and ATP-binding motifs (A, B and C boxes). The front 2 helices of the bundle correspond to α-5 and α-6 in this drawing to illustrate the continuity of the polypeptide chain between the TM and ATP-binding domains.

agreement with the composition measured by infrared spectroscopy (Sonveaux et al., 1996). This leaves only the hydrophobic membrane-spanning domains to account for most of the 26% β-structure.

A recent report of electron microscopy image analysis determined the structure of Pgp to 2.5 nm resolution (Rosenberg et al., 1997). An analysis of single particles by averaging of multiple images showed that at the extracellular surface, Pgp molecules presented a 7 nm diameter toroidal structure with a central 5 nm aqueous pore. The pore narrows to a diameter of 2.5 nm within the membrane. The authors interpreted the unprocessed electron micrograph images as indicating that each molecule consisted of only one pore. However, pairs of aqueous pores are clearly visible in the electron micrographs, and our proposal of two pores (β-barrels) per molecule is consistent with the diameter of each pore derived from image averaging (7 nm) and with the dimensions of the unit cell (14 × 18 nm) derived from the Fourier analysis of crystalline arrays of Pgp molecules. This proposal is also supported by the rectangular shape of the side-on view, as revealed in the image produced from the crystalline arrays. The appearance of isolated single pores in the electron micrographs could be explained by the existence of a closed conformation of the barrel, since the open pores were only visible by a negative staining process. Alternatively, the apposition of the two halves of the molecule may have been ruptured during the processing and fixation of the protein, with the two halves remaining connected by the linker region. Indeed, this interpretation might explain the existence of small satellite features, disconnected from the main body of the molecule, seen in the 3-D reconstruction. Two lobes on the cytoplasmic side of the molecule are designated as NBDs (Rosenberg et al., 1997), but could instead correspond to one helix bundle beneath the β-barrel (our model) and one NBD. The asymmetric disposition of these lobes supports this interpretation.

Several examples have appeared in the recent literature of proposed or revised topologies of membrane proteins that are now thought to contain β-sheet and α-helical composite structures. GLUT1 has recently been revised from analyses of the hydropathy and circular dichroism profiles, amphiphilicity and turn propensity to suggest a largely β-sheet topology that may fold as a β-barrel (Fischbarg et al., 1993). An alternative topological model has been proposed for the OmpA porin (Stathopoulos, 1996), with Raman spectroscopy and computer predictions suggesting that a portion of the C-terminal half may adopt an α-helical conformation and be located inside the β-barrel. Studies of the nicotinic acetylcholine receptor using infrared spectroscopy revealed that the protease-resistant TM domain was 50% α-helical, 40% β-strands and turns, and 10% random coil (Gorne-Tschelnokow et al., 1994). This composition contradicts previous secondary structure α-helical models for this molecule that were based solely on the hydropathy plot. Moreover, a 9 Å resolution structure obtained by electron microscopy indicated that 4 helices resided within the central pore of the membrane channel. These helices are enclosed on the lipid-facing side by a continuous rim of electron density that is insufficient to represent α-helices that could form a β-sheet structure (Unwin, 1995). A Fourier transform infrared spectroscopy study of the secondary structure of the H^+,K^+-ATPase yielded 35% α-helices, 35% β-sheets, 20% turns and 15% random coils (Raussens et al., 1997). The authors draw an analogy with porins on the basis of: (i) the lack of distinct infrared linear dichroism that is typical of porin β-sheets; (ii) the rapid amide hydrogen/deuterium exchange rate that is atypical of bacteriorhodopsin and suggests the presence of a membrane pore or channel; and (iii) an indication of at least 12 porin-like β-sheets when the primary amino acid sequence was analyzed with a β-sheet prediction algorithm. Because the spectroscopy also detected extensive TM α-helical structure, the authors did not propose a model for the membrane topology, though they did note the unreliability of using hydropathy plots and the bacteriorhodopsin model for structure predictions (Raussens et al., 1997). Recent low resolution electron crystallography images of the related H^+-ATPase were interpreted as showing the transmem-

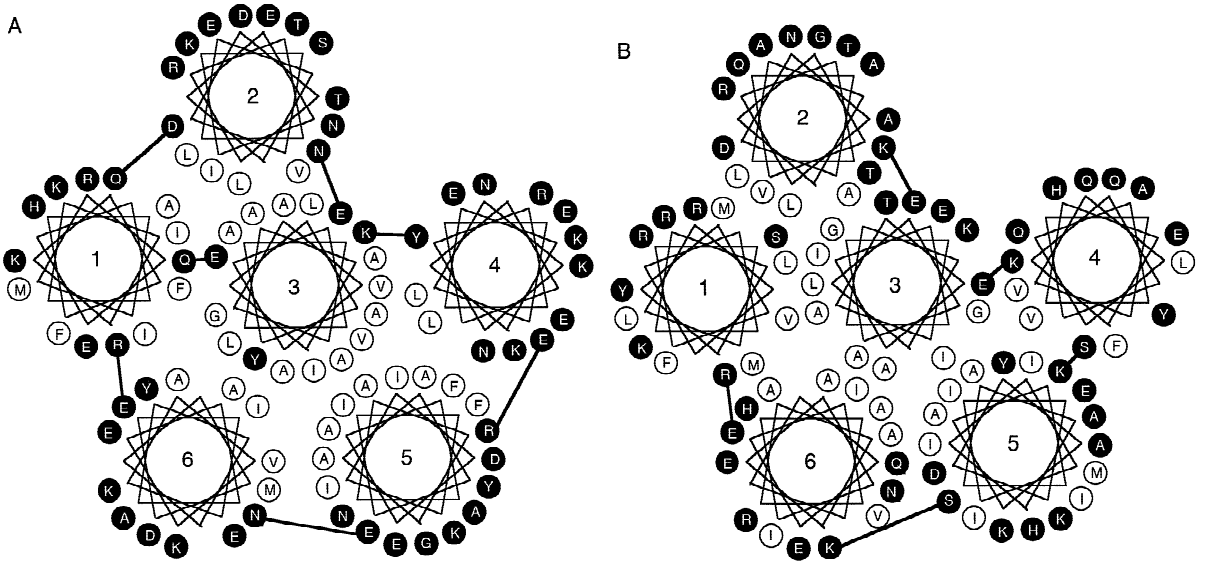

Fig. 5. Helical wheel representation of the 6-helix bundles in each half of MDR1. The standard one letter code for amino acids is used, with hydrophilic residues shaded. Bars indicate potential salt bridges between residues at the same vertical distance — or within one pitch length — from the top of the helix bundle. The pattern of polarity and contact points for these helices is preserved in all other Pgp isoforms (not shown). Panels *A* and *B* are the N- and C-terminal bundles, respectively.

brane domains as entirely α-helical (Auer, Scarborough & Kuhlbrandt, 1998).

Mapping Evidence is Consistent with a β-barrel Topology for P-glycoprotein

Loo and Clarke (1995) constructed a cysteine-less mutant of human Pgp, then inserted cysteines singly at 14 different positions in the predicted extracellular and cytoplasmic loops of the molecule, creating functional mutants in which the position of each cysteine substitution could be determined using membrane-permeant and impermeant thiol-specific reagents. Six substitutions on the putative extracellular loops between TMs 3 and 4 (T209C, G211C, T215C) and TMs 9 and 10 (S850C, G854C, W855C) unexpectedly failed to react with the labeling reagent. These loops deserve some consideration, since we predict them inside while the original proposal has them outside. The unreactivity of these substitutions was explained by the suggestion that these two short loops reside predominantly within the lipid bilayer and are thereby inaccessible to the membrane-permeant labeling reagent (Loo & Clarke, 1995). In our model (Fig. 3), these six residues are situated in the cytoplasm on the inner face of the membrane, between β-8N and β-9N and β-8C and β-9C respectively. These substitutions failed to react with the membrane-permeant labeling reagent, presumably due to steric inaccessibility which would be more likely at the intracellular (our model) rather than extracellular (6 + 6 model) membrane surface. All of the other cysteine mutants (Loo & Clarke, 1995) are positioned correctly in both models according to their relative reactivity. Studies using truncated hamster Pgp1 molecules (Zhang, Collins & Greenberger, 1995) have shown that R207 and K210 (equivalent to R210 and K213, MDR1) act as topogenic signals and serve to retain the loop joining TMs 3 and 4 (old model) within the cytoplasm, a location consistent with the prediction of the β-barrel model.

Kast et al. (1996) used haemagglutinin epitope tagged insertions and immunofluorescence to detect the positions of the tags. This analysis supported the 6 + 6 TM model, but the 10 epitope map positions obtained from this study are also in good agreement with our model, with the exception of the tag attached to the loop joining TMs 9 and 10 (old model), located extracellularly. The mapping of this loop, however, required a triple tag — amounting to 27 amino acids — and the function of this construct was impaired significantly. Such a large insertion might have affected proper processing and membrane insertion. Indeed, the immunoblots for this mutant clearly indicated the presence of at least two forms of the protein (Kast et al., 1996).

Other studies have attempted to map the membrane topology of Pgp using truncated molecules of Pgp that, in some cases, have been fused to large reporter proteins (Bibi & Beja, 1994; Beja & Bibi 1995; Skach, Calayag & Lingappa, 1993; Zhang & Ling, 1991; Zhang, Duthie & Ling, 1993). While these studies have supported alternative arrangements of Pgp, with one or more of the putative TMs deployed to one or other side of the membrane, it has been argued that in view of the sensitivity of Pgp folding to even small changes in the molecule, only

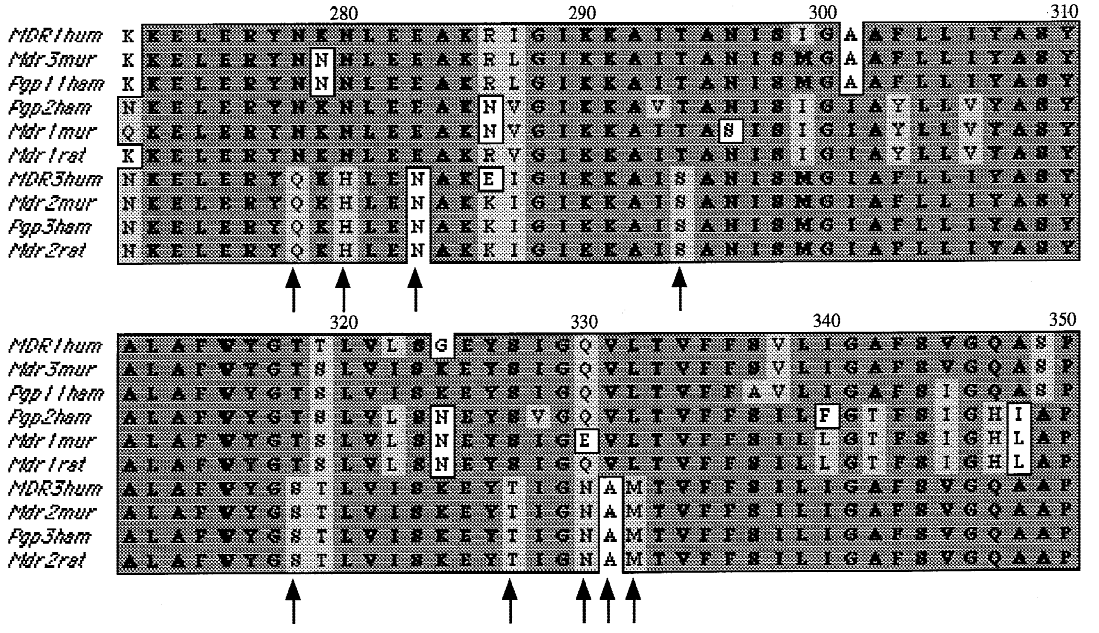

Fig. 6. Partial amino acid sequence alignment of ten Pgp isoforms. The ten isoforms are listed in decreasing order of identity with human MDR1 at the top. The first six isoforms are true Mdrs and the bottom four are non-Mdrs. Identical residues are on a dark grey background; conserved residues are backed by light grey; and non-conserved residues are on a white background. Numbers refer to the residue positions in human MDR1. Arrows indicate positions of identical residues in the bottom four non-Mdrs.

studies involving functional molecules can be considered valid (Loo & Clarke, 1996). With this in mind, one result from these alternative topological studies demands particular attention. Bibi & Beja (1994) constructed a hybrid protein in which an alkaline phosphatase reporter polypeptide was inserted between L226 and S227 in the complete murine Mdr1 molecule. This result indicated an extracellular location for this site, and this sandwich hybrid Mdr1 was shown subsequently to be functional (Beja & Bibi 1995). In the β-barrel model, this site (L226–S227) occurs within the extracellular loop connecting the β-9 and β-10 strands in the N-terminal half of Pgp (Fig. 3), and would thus not necessarily cause disruption to the transmembrane structure of the Pgp molecule. In the 6 + 6 model, however, this large insertion would be positioned in the middle of TM4.

Multiple Sequence Alignment of P-glycoproteins Delineates Mdr and Non-Mdr Classes and Identifies Potential Drug Binding and Translocation Regions

We examined a ClustalW alignment of 10 Pgp isoforms for features that might support our model. Part of this alignment is depicted in Fig. 6, in which the isoforms are listed in descending order of identity with human MDR1 at the top. The first 6 isoforms are true Mdrs — that is they efflux a range of substrates — whereas the bottom 4 isoforms are non-Mdrs that are presumed to transport a single substrate or substrates of a single class. The arrows in Fig. 6 indicate identical residues for all 4 non-Mdrs, and a different residue(s) for the top 6 Mdrs. In all, there are 169 of these positional differences in the complete amino acid sequences of the 10 isoforms. Ignoring the N-terminus and the linker region between the two homologous halves of the molecules that are known not to be involved in drug binding (Devault & Gros, 1990), all of the remaining differences are plotted as black dots on the secondary structural model for Pgp (Fig. 7). The remarkable result of this exercise is that all of the residues are positioned on loops and turns that contribute to the topologies of proposed drug binding and translocating sites; and that the structural scaffolding remains largely unaffected by the residue differences that delineate the Mdr and non-Mdr isoforms. Residues known to affect substrate utilization were also plotted on the secondary structural model (Fig. 7; open and shaded circles; referenced in the legend). Significantly, like the result for the residues that delineate the Mdr/non-Mdr categories, none of the residues that affected substrate utilization were located within the structural scaffolding of the model, that is, the TM β-strands and cytoplasmic helix bundles. In addition, there are numerous substitutions that have little or no effect on substrate specificity (*see* references in the legend to Fig. 7). These mutations are scattered throughout the Pgp molecule in no discernible pattern in relation to

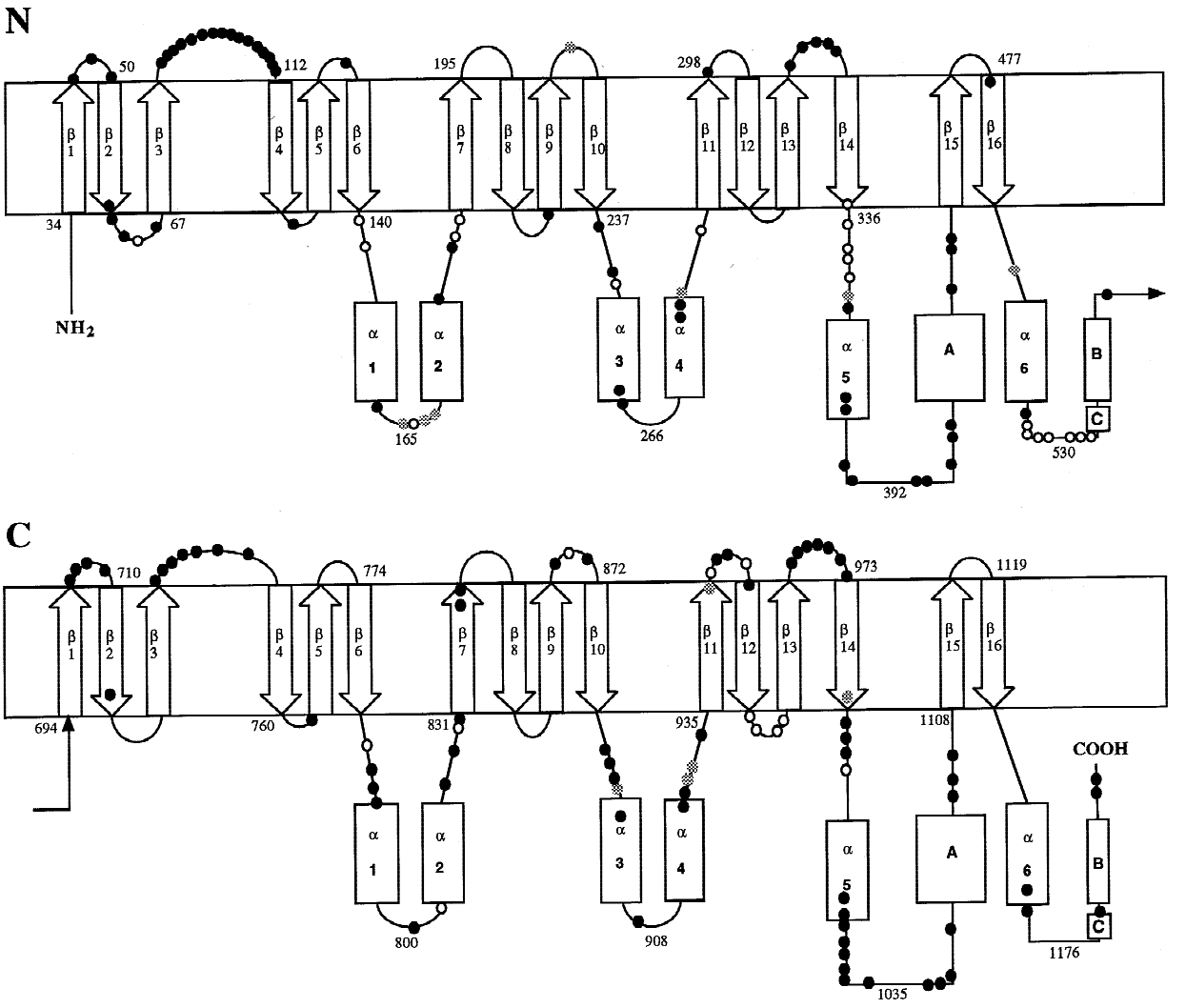

Fig. 7. Distribution of amino acid changes in Mdr and non-Mdr Pgp isoforms on the new topological model. The N- (panel N) and C-terminal halves (panel *C*) of human MDR1 deploy sixteen TM beta-sheets (arrowed rectangles) and six cytoplasmic alpha-helices (rectangles), with numbers giving sequential coordinates through the molecule. The lettered boxes A, B and C, and associated loops represent the ATP domains. Black filled-in circles indicate residues that are identical in the four non-Mdrs but different in the six true Mdrs (this study); open circles indicate residues known to affect substrate utilization; and grey filled-in circles indicate the overlap residues of the two categories. The residues that affected substrate utilization were obtained from references: Choi et al., (1988); Currier et al., (1992); Chir et al., (1993); Loo & Clarke (1993*a; b;* 1994*a; b*); Hanna et al., (1996); Taguchi et al., (1997); and Bakos et al., (1997).

our model. Some of these lie within putative TM β-strands 7N, 9N, 14N, 5C, 6C, 8C, 11C and 12C. When the Mdr/non-Mdr residues and those that affect substrate utilisation are plotted on the current 6 + 6 helix Pgp model, 28/134 or 21% were scattered within many of the TM helices and loops and turns (Fig. 8).

The clustering of residues on the loops joining the helix bundle to the transmembrane barrel and on the turns joining TM β-strands, leads us to suggest that these loops may act to bind and facilitate the translocation of substrates, by folding into the barrel lumen in a manner analogous to porins and other transporters. While the intracellular loops may act to bind and efflux substrate, the extracellular loops connecting the TM β-strands may act to facilitate the exit of the substrate from the transmembrane channel, or perhaps even act to reduce drug influx by binding substrate directly from the extracellular space. Evidence supporting this proposed mechanism comes from a recent report of experiments on highly purified Pgp using $^{2}H/H$ exchange kinetics (Sonveaux et al., 1996). This analysis revealed that Pgp undergoes profound conformational changes resulting in increased solvent accessibility for at least 75 amino acids upon addition of MgATP, while addition of MgATP plus the substrate verapamil resulted in decreased solvent accessibility for at least 102 amino acids.

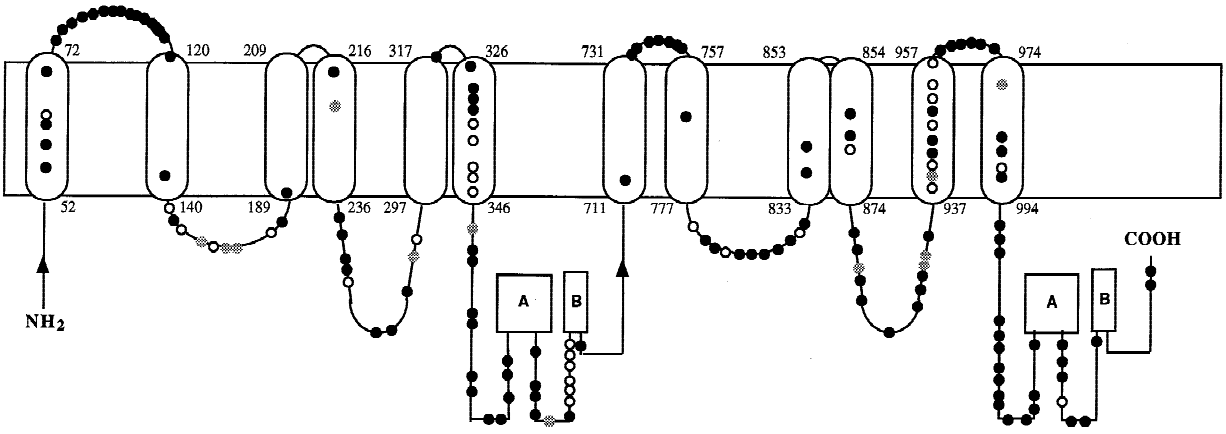

Fig. 8. Distribution of amino acid changes in Mdr and non-Mdr Pgp isoforms on the current topological model. The twelve TM helices are depicted as lozenges with numbers representing residue positions at either end of each TM helix. The ATP domains are represented as Walker A and B motifs and associated loops. Circle designations are described in the legend to Fig. 7.

Loo & Clarke (1997) introduced pairs of cysteine residues into putative TMs 6 and 12 and demonstrated a pattern of oxidative cross-linking that was consistent with the TMs being arranged in a left-handed coiled coil. Four cross-linked pairs, namely L332C/L975C, F343C/M986C, G346C/G989C and P350C/S993C, were generated in separate mutant molecules. The cross-linking of the last three of these pairs was blocked by drug substrates, unaffected by ATP and reversed by dithiothreitol. In our model, these three pairs are positioned on the connecting loops directly below the β-14 strands in each half of the model (Figs. 2 and 3). Cross-linking of P350C to S993C severely impaired drug-stimulated ATPase activity, suggesting that the two regions of which they are components must be free to move independently for proper function. Thus in our model, the two β-14 strands and the loops below would be adjacent to one another. The cross-linking of the first pair (L332C/L975C) required the presence of ATP, was unaffected by drug substrates, and could not be reversed by treatment with dithiothreitol. This pair is at the top of the β-14 strands near the extracellular loops, and since the crossed-linking of this pair is the only one that required ATP hydrolysis, we suggest that a conformational shift might be necessary to bring the side chains of these two residues together. In contrast, two other potential pairs that lie between the first and second of the four cross-linked pairs within TMs 6 and 12 (Loo & Clarke, 1997), namely F336C/S979C and L339C/V982C, failed to form cross-links. In our model, these residues lie within the β-14 strands and their side chains may not face one another and may be unable to cross-link.

Kinetic studies (Stein et al., 1994) suggested that Pgp plays a role in both reducing drug influx and increasing drug efflux, and that these are functionally distinct processes. Pgp could reduce drug influx by binding or collecting substrate at the extracellular loops and within the lumen of the barrels, directly from the extracellular space. This collection feature would explain why substrates normally partitioned in the membranes of drug-sensitive cells, are found only associated with Pgp in the membranes of drug-resistant cells (Raviv et al., 1990). Also consistent with this proposal is the observation that the Pgp substrate rhodamine 123 has a fluorescence excitation spectrum in drug-sensitive cells similar to its spectrum in octanol, indicating its probable location in the membrane, while in drug-resistant cells the spectrum is intermediate between this and its aqueous spectrum (Kessel, 1989), which could be explained by its probable location with the intermediate hydrophobicity of the β-barrels and its associated loops. The results of these and many other experiments (reviewed in Germann, 1996) have led to the hypothesis that Pgp binds its substrates from with the membrane. More recently, studies using Pgp substrates that fluoresce when membrane-bound, have been interpreted as showing that Pgp translocate these substrates from the cytoplasmic leaflet of the lipid bilayer, directly to the extracellular space (Shapiro & Ling, 1997, 1998; Shapiro, Corder & Ling, 1997). These data, however, do not require that the binding site for these substrates is located within the membranes. The specific initial rate of transport was found to be directly proportional to the amount of membrane-bound substrate and inversely proportional to the concentration of free, aqueous substrate. Since the rate of passive re-equilibration of lipid-bound substrates to the external aqueous phase was shown to be rapid with respect to the rate of active transport, it is also possible that the binding pocket for these substrates is located within the cytoplasm, with access to the surface of the membrane but not to the cytoplasm.

Origin of P-glycoprotein and other ABC Transporters

The low sequence homology among the bacterial porins suggests that rather than forming a narrow clade, these molecules may have evolved to be part of a much wider spectrum of membrane proteins than is currently known. In evolutionary terms, it is easier to explain the development of transporters if a common translocation unit was conserved and different loops evolved for different functions (Fischbarg et al., 1994). A predictive analysis of bacterial transporters of several families with common structural motifs (Nikaido & Saier, 1992) suggests a central membrane translocation unit onto which an energy coupling component may have been grafted evolutionarily. Could Pgp and progenitors of other ABC transporters have derived from the fusion of genes for passive channel-forming porins and membrane-associated ATPases, with conserved features of the original proteins that identify extant component porin and ATPase domains?

We thank Tom Ferenci, Department of Microbiology, University of Sydney, for helpful comments. This work was supported by grants from the Baxter Perpetual Charitable Trust and the R.G. Arnott Foundation.

References

Auer, M., Scarborough, G.A. Kühlbrandt, W. 1998. Three-dimensional map of the plasma membrane H^+-ATPase in the open conformation. *Nature* **392:**840–843

Bakos, E., Klein, I., Welker, E., Szabo, K., Muller, M., Sarkadi, B., Varadi, A. 1997. Characterization of the human multidrug resistance protein containing mutations in the ATP-binding cassette signature region. *Biochem. J.* **323:**773–783

Beja, O., Bibi, E. 1995. Multidrug resistance protein (Mdr)-alkaline phosphatase hybrids in *Escherichia coli* suggest a major revision in the topology of the C-terminal half of Mdr. *J. Biol. Chem.* **270:**12351–12354

Bibi, E., Beja, O. 1994. Membrane topology of multidrug resistance protein expressed in *Escherichia coli*. *J. Biol. Chem.* **269:**19910–19915

Blattner, F.R., Plunket III, G. Bloch, C.A., Perna, N.T., Burland, V., Riley, M., Collado-Vides, J., Glasner, J.D., Rode, C.K., Mayhew, G.F., Gregor, J., Davis, N.W., Kirkpatrick, H.A., Goeden, M.A., Rose, D.J., Mau, B., Shao, Y. 1997. The complete genome sequence of *Escherichia coli* K-12. *Science* **277:**1453–1474

Bolhuis, H., van Veen, H.W., Poolman, B., Driessen, A.J.M., Konings, W.N. 1997. Mechanisms of multidrug transporters. *FEMS Microbiol. Rev.* **21:**55–84

Choi, K., Chen, C-J., Kriegler, M., Roninson, I.B. 1988. An altered pattern of cross-resistance in multidrug-resistant human cells results from spontaneous mutations in the *mdr1* (P-glycoprotein) gene. *Cell* **53:**519–529

Chou, P.Y., Fasman, G.D. 1973. Structure and functional role of leucine residues in proteins. *J. Mol. Biol.* **74:**263–281

Cowan, S.W., Rosenbusch, J.P. 1994. Folding pattern diversity of integral membrane proteins. *Science* **264:**914–916

Cowan, S.W., Schirmer, T., Rummel, G., Steiert, M., Ghosh, R., Paupit, R.A., Jansonius, J.N., Rosenbusch, J.P. 1992. Crystal structures explain functional properties of two *E. coli* porins. *Nature* **358:**727–733

Currier, S.J., Kane, S.E., Willingham, M.C., Cardarelli, C.O., Pastan, I., Gottesman, M.M. 1992. Identification of residues in the first cytoplasmic loop of P-glycoprotein involved in the function of chimeric human MDR1-MDR2 transporters. *J. Biol Chem.* **267:**25153–25159

Deber, C.M., Glibowicka, M., Woolley, G.A. 1990. Conformations of proline residues in membrane environments. *Biopolymers* **29:**149–157

Devault, A., Gros, P. 1990. Two members of the mouse mdr gene family confer multidrug resistance with overlapping but distinct drug specificities. *Mol. Cell. Biol.* **10:**1652–1663

Dhir, R., Grizzuti, K., Kajiji, S., Gros, P. 1993. Modulatory effects on substrate specificity of independent mutations at the serine 939/941 position in predicted transmembrane domain 11 of P-glycoprotein. *Biochemistry* **32:**9492–9499

Endicott, J.A., Ling, V. 1989. The biochemistry of P-glycoprotein-mediated drug resistance. *Annu. Rev. Biochem.* **58:**137–171

Ferenci, T. 1989. Is hydrophobicity analysis sufficient to predict topography of membrane proteins? *Trends Biochem. Sci.* **14:**96

Fischbarg, J., Cheung, M., Czegledy, F., Li, J., Iserovich, P., Kuang, K., Hubbard, J., Garner, M., Rosen, O.M., Golde, D.W., Vera, J.C. 1993. Evidence that facilitative glucose transporters may fold as β-barrels. *Proc. Natl. Acad. Sci. USA* **90:**11658–11662

Fischbarg, J., Cheung, M., Li, J., Iserovitch, P., Czegledy, F., Kuang, K., Garner, M. 1994. Are most transporters and channels beta barrels? *Mol. Cell. Biochem.* **140:**147–162

George, A.M., Davey, M.W., Mir, A.A. 1996. Functional expression of the human *MDR1* gene in *Escherichia coli*. *Arch. Biochem. Biophys.* **333:**66–74

Geourjon, C., Deleage, G. 1994. SOPM: A self optimised prediction method for protein secondary structure prediction. *Protein Eng.* **7:**157–164

Geourjon, C., Deleage, G. 1995. Significant improvements in protein secondary structure prediction by prediction from multiple alignments. *CABIOS* **11:**681–684

Germann, U.A. 1996. P-glycoprotein — A mediator of multidrug resistance in tumour cells. *Eur. J. Cancer* **32A:**927–944

Gorne-Tschelnokow, U., Strecker, A., Kaduk, C., Naumann, D., Hucho, F. 1994. The transmembrane domains of the nicotinic acetylcholine receptor contain α-helical and β structures. *EMBO. J.* **13:**338–341

Gottesman, M.M., Hrycyna, C.A., Schoenlein, P.V., Germann, U.A., Pastan, I. 1995. Genetic analysis of the multidrug transporter. *Annu. Rev. Genetics* **29:**607–649

Gottesman, M.M., Pastan, I. 1993. Biochemistry of multidrug resistance mediated by the multidrug transporter. *Annu. Rev. Biochem.* **62:**385–427

Hanna, M., Brault, M. Kwan, T., Kast, C., Gros, P. 1996. Mutagenesis of transmembrane domain 11 of P-glycoprotein by alanine scanning. *Biochemistry* **35:**3625–3635

Higgins, C.F. 1995. The ABC of channel regulation. *Cell* **82:**693–696

Higgins, C.F. 1992. ABC transporters: from microorganisms to man. *Annu. Rev. Cell Biol.* **8:**67–113

Hoedemaeker, F.J., Davidson, A.R., Rose, D.R. 1998. A model for the nucleotide-binding domains of ABC transporters based on

the large domain of aspartate aminotransferase. Proteins **30:**275–286

Hyde, S.C., Emsley, P., Hartshorn, M.J., Mimmack, M.M., Gileadi, U., Pearce, S.R., Gallagher, M.P., Gill, D.R., Hubbard, R.E., Higgins, C.F. 1990. Structural model of ATP-binding proteins associated with cystic fibrosis, multidrug resistance, and bacterial transport. *Nature* **346:**362–365

Juliano, R.L., Ling, V. 1976. A surface glycoprotein modulating drug permeability in Chinese hamster ovary cell mutants. *Biochim. Biophys. Acta* **455:**152–162

Juranka, P.F., Zastawny, R.L., Ling, V. 1989. P-glycoprotein: multidrug-resistance and a superfamily of membrane-associated transport proteins. *FASEB. J.* **3:**2583–2592

Kane, S.E. 1996. Multidrug resistance of cancer cells. *Adv. Drug Res.* **28:**182–252

Kast, C., Canfield, V., Levenson, R., Gros, P. 1996. Transmembrane organization of mouse P-glycoprotein determined by epitope insertion and immunofluorescence. *J. Biol. Chem.* **271:**9240–9248

Kessel, D. 1989. Exploring multidrug resistance by using rhodamine 123. *Cancer Commun.* **1:**145–149

Kyte, J., Doolittle, R.F. 1982. A simple method for displaying the hydropathic character of a protein. *J. Mol. Biol.* **157:**105–132

Loo, T.W., Clarke, D.M. 1993*a*. Functional consequences of proline mutations in the predicted transmembrane domain of P-glycoprotein. *J. Biol. Chem.* **268:**3143–3149

Loo, T.W., Clarke, D.M. 1993*b*. Functional consequences of phenylalanine mutations in the predicted transmembrane domain of P-glycoprotein. *J. Biol. Chem.* **268:**19965–19972

Loo, T.W., Clarke, D.M. 1994*a*. Functional consequences of glycine mutations in the predicted cytoplasmic loops of P-glycoprotein. *J. Biol. Chem.* **269:**7243–7248

Loo, T.W., Clarke, D.M. 1994*b*. Mutations to amino acids located in predicted transmembrane segment 6 (TM6) modulate the activity and substrate specificity of human P-glycoprotein. *Biochemistry* **33:**14049–14057

Loo, T.W., Clarke, D.M. 1995. Membrane topology of a cysteine-less mutant of human P-glycoprotein. *J. Biol. Chem.* **270:**843–848

Loo, T.W., Clarke, D.M. 1996. Mutational analysis of the predicted first transmembrane segment of each homologous half of human P-glycoprotein suggests that they are symmetrically arranged in the membrane. *J. Biol. Chem.* **271:**15414–15419

Loo, T.W., Clarke, D.M. 1997. Drug-stimulated ATPase activity of human P-glycoprotein requires movement between transmembrane segments 6 and 12. *J. Biol. Chem.* **272:**20986–20989

Mehta, P.K., Heringa, J., Argos, P. 1995. A simple and fast approach to prediction of protein secondary structure from multiply aligned sequences with accuracy above 70%. *Protein Sci.* **4:**2517–2525

Mimura, C.S., Holbrook, S.R., Ames, G.F-L. 1991. Structural model of the nucleotide-binding conserved component of periplasmic permeases. *Proc. Natl. Acad. Sci. USA* **88:**84–88

Nikaido, H., Saier, Jr. M.H. 1992. Transport proteins in bacteria: Common themes in their design. *Science* **258:**936–942

Pawagi, A.B., Wang, J., Silverman, M., Reithmeier, A.F., Deber, C.M. 1994. Transmembrane aromatic amino acid distribution in P-glycoprotein. *J. Mol. Biol.* **235:**554–564

Raussens, V., Ruysschaert, J-M., Goormaghtigh, E. 1997. Fourier transform infrared spectroscopy study of the secondary structure of the gastric H^+,K^+-ATPase and of its membrane-associated proteolytic peptides. *J. Biol. Chem.* **272:**262–270

Raviv, Y., Pollard, H.B., Bruggemann, E.P., Pastan, I., Gottesman, M.M. 1990. Photosensitised labeling of a functional multidrug transporter in living drug-resistant tumor cells. *J. Biol. Chem.* **265:**3975–3980

Rosenberg, M.F., Callaghan, R., Ford, R.C., Higgins, C.F. 1997. Structure of the multidrug resistance P-glycoprotein to 2.5 nm resolution determined by electron microscopy and image analysis. *J. Biol. Chem.* **272:**10685–10694

Rost, B., Sander, C. 1993. Prediction of protein structure at better than 70% accuracy. *J. Mol. Biol.* **232:**584–599

Rost, B., Sander, C. 1994. Conservation and prediction of solvent accessibility in protein families. *Proteins* **20:**216–226

Ruetz, S., Gros, P. 1994. A mechanism for P-glycoprotein action in multidrug resistance: are we there yet? *Trends Pharmacol. Sci.* **15:**260–263

Salamov, A.A., Solovyev, V.V. 1995. Prediction of protein secondary structure by combining nearest-neighbor algorithms and multiple sequence alignments. *J. Mol. Biol.* **247:**11–15

Schirmer, T., Cowan, S.W. 1993. Prediction of membrane-spanning β-strands and its application to maltoprotein. *Protein Sci.* **2:**1361–1363

Schirmer, T., Keller, T.A., Wang, Y-F., Rosenbusch, J.P. 1995. Structural basis for sugar translocation through maltoprotein channels at 3.1 Å resolution. *Science* **267:**512–541

Shapiro, A.B., Corder, AB., Ling, V. 1997. P-glycoprotein-mediated Hoechst 33342 transport out of the lipid bilayer. *Eur. J. Biochem.* **250:**115–121

Shapiro, A.B., Ling, V. 1997. Extraction of Hoechst 33342 from the cytoplasmic leaflet of the plasma membrane by P-glycoprotein. *Eur. J. Biochem.* **250:**122–129

Shapiro, A.B., Ling, V. 1998. Transport of LDS-751 from the cytoplasmic leaflet of the plasma membrane by the rhodamine-123-selective site of P-glycoprotein. *Eur. J Biochem.* **254:**181–188

Skach, W.R., Calayag, M.C., Lingappa, V.R. 1993. Evidence for an alternate model of human P-glycoprotein structure and biogenesis. *J. Biol. Chem.* **268:**6903–6908

Solovyev, V., Salamov, A.A. 1994. Predicting α-helix and β-strand segments of globular proteins. *CABIOS* **10:**661–669

Song, L., Hobaugh, M.R., Shustak, C., Cheley, S., Bayley, H., Gouaux, J.E. 1996. Structure of staphylococcal α-hemolysin, a heptameric transmembrane pore. *Science* **274:**1859–1866

Sonveaux, N., Shapiro, A.B., Goormaghtigh, E., Ling, V., Ruysschaert, J.M. 1996. Secondary and tertiary structure changes of reconstituted P-glycoprotein — a fourier transform attenuated total reflection infrared spectroscopy analysis. *J. Biol. Chem.* **271:**24617–24624

Stathopoulos, C. 1996. An alternative topological model for *Escherichia coli* OmpA. *Protein Sci.* **5:**170–173

Stein, W.D., Cardarelli, C.O., Pastan, I., Gottesman, M.M. 1994. Kinetic evidence suggesting that the multidrug transporter differentially handles influx and efflux of its substrates. *Mol. Pharmacol.* **45:**763–772

Stultz, C.M., White, J.V., Smith, T.F. 1993. Structural analysis based on state-space modeling. *Protein Sci.* **2:**305–314

Taguchi, Y., Kino, K., Morishima, M., Komano, T., Kane, S.E., Ueda, K. 1997. Alteration of substrate specificity by mutations at the His^{61} position in predicted transmembrane domain I of human MDR1/P-glycoprotein. *Biochemistry* **36:**8883–8889

Tatusov, R.L., Koonin, E.V., Lipman, D.J. 1997. A genomic perspective on protein families. *Science* **278:**631–637

Thompson, J.D., Higgins, D.G., Gibson, T.J. 1994. Improving the sensitivity of progressive multiple sequence alignment through sequence weighting, positions-specific gap penalties and weight matrix choice. *Nucleic Acids Res.* **22:**4673–4680

Unwin, N. 1995. Acetylcholine receptor channel imaged in the open state. *Nature* **373:**37–43

Van Veen, H.W., Vanema, K., Bolhuis, H. Oussenko, I., Kok, J., Poolman, B., Driessen, A.J.M., Konings, W.N. 1996. Multidrug resistance mediated by a bacterial homolog of the human multi-

drug transporter MDR1. *Proc. Natl. Acad. Sci. USA* **93:**10668–10672

van der Bliek, A.M., Kooiman, P.M., Schneider, C., Borst, P. 1988. Sequence of mdr3 cDNA encoding a human P-glycoprotein. *Gene* **71:**401–411

White, J.V., Stultz, C.M., Smith, T.F. 1994. Protein classification by stochastic modeling and optimal filtering of amino-acid sequences. *Math. Biosci.* **119:**35–75

Zhang, J-T., Duthie, M., Ling, V. 1993. Membrane topology of the N-terminal half of the hamster P-glycoprotein molecule. *J. Biol. Chem.* **268:**15101–15110

Zhang, J-T., Ling, V. 1991. Study of membrane orientation and glycosylated extracellular loops of mouse P-glycoprotein by in vitro translation. *J. Biol. Chem.* **266:**18224–18232

Zhang, X., Collins, K.I., Greenberger, L.M. 1995. Functional evidence that transmembrane 12 and the loop between transmembrane 11 and 12 form part of the drug-binding domain in P-glycoprotein encoded by *MDR1*. *J. Biol Chem.* **270:**5441–5448